© 2016. Published by The Company of Biologists Ltd | Development (2016) 143, 2443-2454 doi:10.1242/dev.130641

RESEARCH ARTICLE

Genome-wide identification of *Tribolium* dorsoventral patterning genes

Dominik Stappert[1,*], Nadine Frey[1,*], Cornelia von Levetzow[2] and Siegfried Roth[1,‡]

ABSTRACT

The gene regulatory network controlling dorsoventral axis formation in insects has undergone drastic evolutionary changes. In *Drosophila*, a stable long-range gradient of Toll signalling specifies ventral cell fates and restricts BMP signalling to the dorsal half of the embryo. In *Tribolium*, however, Toll signalling is transient and only indirectly controls BMP signalling. In order to gain unbiased insights into the *Tribolium* network, we performed comparative transcriptome analyses of embryos with various dorsoventral pattering defects produced by parental RNAi for Toll and BMP signalling components. We also included embryos lacking the mesoderm (produced by *Tc-twist* RNAi) and characterized similarities and differences between *Drosophila* and *Tribolium twist* loss-of-function phenotypes. Using stringent conditions, we identified over 750 differentially expressed genes and analysed a subset with altered expression in more than one knockdown condition. We found new genes with localized expression and showed that conserved genes frequently possess earlier and stronger phenotypes than their *Drosophila* orthologues. For example, the leucine-rich repeat (LRR) protein Tartan, which has only a minor influence on nervous system development in *Drosophila*, is essential for early neurogenesis in *Tribolium* and the *Tc*-zinc-finger homeodomain protein 1 (Tc-zfh1), the orthologue of which plays a minor role in *Drosophila* muscle development, is essential for maintaining early *Tc-twist* expression, indicating an important function for mesoderm specification.

KEY WORDS: Transcriptome analysis, Toll/NF-κB signalling, BMP signalling, FGF signalling, *twist*, Gastrulation

INTRODUCTION

In the fruit fly, *Drosophila melanogaster*, Toll signalling is crucial for both dorsoventral (DV) axis formation and innate immunity (Leulier and Lemaitre, 2008; Stein and Stevens, 2014). Although the immune function of Toll is conserved from flies to vertebrates, a DV patterning function of Toll has not been observed outside the insects. Indeed, analysis of DV patterning in more basally branching insects indicates that during insect evolution Toll signalling progressively gained the complex morphogen function found in modern flies (Lynch and Roth, 2011; Özüak et al., 2014; Sachs et al., 2015). The red flour beetle *Tribolium castaneum* provides an interesting intermediate position within this evolutionary series. In both *Drosophila* and *Tribolium*, Toll signalling leads to the formation of a ventral-to-dorsal nuclear gradient of the NF-κB transcription factor Dorsal. The NF-κB/Dorsal gradient is fairly stable in *Drosophila* and patterns the DV axis by activating or repressing target genes in a concentration-dependent manner (Hong et al., 2008; Ozdemir et al., 2014; Reeves and Stathopoulos, 2009; Reeves et al., 2012; Roth et al., 1989; Rushlow et al., 1989; Steward, 1989). Among the targets of NF-κB/Dorsal are transcription factors directly involved in cell fate specification such as *twist* (*twi*), as well as components of other signalling pathways which indirectly specify subregions along the DV axis. In particular, the NF-κB/Dorsal gradient tightly controls a number of BMP pathway components, such as the secreted BMP inhibitor *short gastrulation* (*sog*) and the BMP ligand *decapentaplegic* (*dpp*), and thereby initiates the formation of a BMP signalling gradient which specifies dorsal cell fates (Francois et al., 1994; Jazwinska et al., 1999; O'Connor et al., 2006; Wang and Ferguson, 2005). Thus, Toll signalling in *Drosophila* uses multiple mechanisms to provide stable patterning information for the entire DV axis.

In contrast to the situation in *Drosophila*, Toll signalling in *Tribolium* is dynamic. The NF-κB/Dorsal gradient is initiated in a broad domain that then rapidly refines and disappears while the expression domains of potential target genes are established (Chen et al., 2000; Nunes da Fonseca et al., 2008). The number of genes controlled by Toll signalling in *Tribolium* appears to be reduced compared with *Drosophila*. For example, we have not found genes that are repressed by Tc-NF-κB/Dorsal and only one mechanism, the ventral activation of *Tc-sog*, is employed to polarize BMP signalling (van der Zee et al., 2006). BMP signalling appears to play a larger role in DV patterning than in *Drosophila* (Nunes da Fonseca et al., 2010; van der Zee et al., 2006). This is even more pronounced in more basally branching insects. In the jewel wasp *Nasonia vitripennis*, representing the Hymenoptera (the outgroup to all other holometabolous insects), BMP patterns the entire axis, whereas Toll is only required locally to induce mesoderm formation (Özüak et al., 2014). In the milkweed bug *Oncopeltus fasciatus* (a hemimetabolous insect), Toll lacks all instructive roles for tissue specification; it only polarizes BMP signalling, which in turn patterns the DV axis (Sachs et al., 2015). Taken together, the DV gene regulatory network (GRN) of *Tribolium* deviates from that of *Drosophila* in many interesting ways, but has not diverged as much as the DV-GRN of more basally branching insects, making it a preferable choice for direct molecular comparisons with *Drosophila*.

Aside from the attractive intermediate position of its DV-GRN, *Tribolium* offers a number of additional advantages. First, *Tribolium* development shares many features with other insects (including species from basal lineages), which are absent or highly modified in *Drosophila*, e.g. the short-germ mode segmentation and the presence of two complete extraembryonic membranes, serosa and amnion, instead of a reduced amnioserosa (Beermann and Schröder, 2008). Second, *Tribolium* provides many tools for

[1]Institute of Developmental Biology, Biocenter, Zuelpicher Str. 47b, University of Cologne, Cologne 50674, Germany. [2]Centrum für Integrierte Onkologie (CIO) Köln Bonn, Universitätsklinikum Köln, Kerpener Str. 62, Köln 50937, Germany.
*These authors contributed equally to this work

‡Author for correspondence (siegfried.roth@uni-koeln.de)

S.R., 0000-0001-5772-3558

Received 6 October 2015; Accepted 19 May 2016

Development (2016) 143, 2443-2454 doi:10.1242/dev.130641

functional studies. It possesses a particularly strong systemic RNAi response – which was the basis for a recent genome-wide RNAi screen (Schmitt-Engel et al., 2015) – and techniques for forward genetic screens, transgenesis and live imaging are available (Benton et al., 2013; Berghammer et al., 1999, 2009; Koelzer et al., 2014; Sarrazin et al., 2012). Therefore, we have chosen *Tribolium* for unbiased genomic approaches like ChIP-seq (D. Stappert, Two novel, complementary next generation sequencing approaches to reveal the dorso-ventral gene regulatory network of *Tribolium castaneum*. PhD Thesis, University of Cologne, 2014) and RNA-seq, which should enable us to reconstruct the *Tribolium* DV-GRN for a thorough comparison with *Drosophila* and more basally branching insects. Here, we describe the results of RNA-seq experiments that compare transcriptomes of strongly ventralized or dorsalized embryos generated by knockdown of key DV patterning genes by parental RNAi. We also include embryos lacking only the mesoderm generated by *Tc-twi* RNAi and, for the first time, provide a thorough description of the *Tc-twi* knockdown phenotype.

RESULTS

We used four highly penetrant knockdown conditions to produce narrowly staged embryos with DV defects for transcriptome analysis (Fig. 1; Fig. S1). Two conditions were selected to produce severely dorsalized embryos: *Tc-Toll* and *Tc-sog* RNAi. Both lead to a loss of ventral (neuroectodermal) and an expansion of dorsal ectodermal cell fates. However, only *Tc-Toll* knockdown yields embryos in which the mesoderm is deleted (apparent from the loss of *Tc-twi* expression; Fig. 1A-C; Fig. S1H,I) (Nunes da Fonseca et al., 2008; van der Zee et al., 2006). One condition was used to produce severely ventralized embryos: *Tc-dpp* RNAi, which results in an expansion of the neuroectoderm at the expense of the dorsal ectoderm (Fig. 1A,D) (van der Zee et al., 2006). In *Tribolium*, DV and anterior-posterior (AP) patterning are more obviously linked than in *Drosophila*, as shown by the fact that the *Tribolium* head anlage occupies a ventral wedge region of the blastoderm and, similarly, the serosa is derived from an anterior-dorsal region of the blastoderm. As a result of this link, dorsalization of embryos reduces the size of the head primordium whereas ventralization causes an expansion (Fig. 1A-D). The only knockdown phenotype used in this study that does not affect AP patterning is that of *Tc-twi* (Fig. 1E).

Tc-twist knockdown results in loss of mesoderm

Whereas a furrow forms along the ventral midline in wild-type embryos (Handel et al., 2005), *Tc-twi* RNAi embryos lack furrow formation (Fig. 2A,B). The tissue along the ventral midline, where *Tc-twi* is usually expressed, seems to be static and appears plate-like from the last mitotic division before gastrulation until germ band extension starts (Movies 1-3) (for staging, see Benton et al., 2013). The germ rudiment around this static plate condenses and the posterior amniotic fold and the head lobes form as in wild-type embryos (Fig. 2A,B; Movies 1-3). During germ band extension, *Tc-twi* RNAi embryos are expanded laterally and are less compact than wild-type embryos (Fig. 2C,D and Movies 1-3). The most obvious morphological difference is observed at the posterior end of fully segmented germ band embryos. In wild-type embryos, the posterior end of the germ band shows the opening of the hindgut (Fig. 2E,G) that extends into the interior and harbours the Malpighian tubules at its anterior end (King and Denholm, 2014). In *Tc-twi* RNAi embryos, the hindgut is detached from its usual location and flipped outwards so that it appears as an external tube connected to the posterior tip of the embryo (Fig. 2F,H). The Malpighian tubules, which are not clearly visible in unstained wild-type embryos, become finger-like protrusions at the tip of this rotated hindgut (Fig. 2E-H).

The lack of the ventral furrow through which mesoderm cells invaginate during gastrulation (Handel et al., 2005) raises the question of whether any cells invaginate and become mesoderm in the absence of *Tc-twi*. Cross sections through anterior regions of gastrulating wild-type embryos show the invaginating mesodermal cells that have lost epithelial organization and are clearly distinct from, and flanked by, the ectodermal epithelium (Fig. 2I). The same is observed in cross sections through posterior regions, although here the number of invaginating cells is larger than anteriorly (Fig. 2K). In sections through *Tc-twi* RNAi embryos, no invaginating cells that lose epithelial organization are present (Fig. 2J,L). This suggests that no mesodermal cells are specified at this stage. Interestingly, the knockdown of *Tc-twi* also seems to influence the structure of the posterior growth zone, as the layer of mesenchymal cells (presumptive mesoderm) that separate the germ cells from the ectoderm is absent after *Tc-twi* knockdown, as shown by sagittal sections through extending germ band embryos (Fig. 2M,N).

As the mesoderm seems to be missing in the *Tc-twist* knockdown embryos and because muscles are mesodermal derivatives, we checked whether muscles are missing after knockdown of *Tc-twi*. To do this, we used the muscle enhancer line pBA19 (Lorenzen et al., 2003). The knockdown of *Tc-twi* in this line resulted in the complete loss of body wall muscles (Fig. 2O,P). In addition, *Tc-twi* knockdown in a cardioblast enhancer line (Koelzer et al., 2014) reveals that the cardioblasts are also lost (Fig. S2).

Taken together, these findings suggest that upon *Tc-twi* knockdown, no mesodermal derivatives form from the ventral-most regions of blastoderm embryos and from the posterior growth

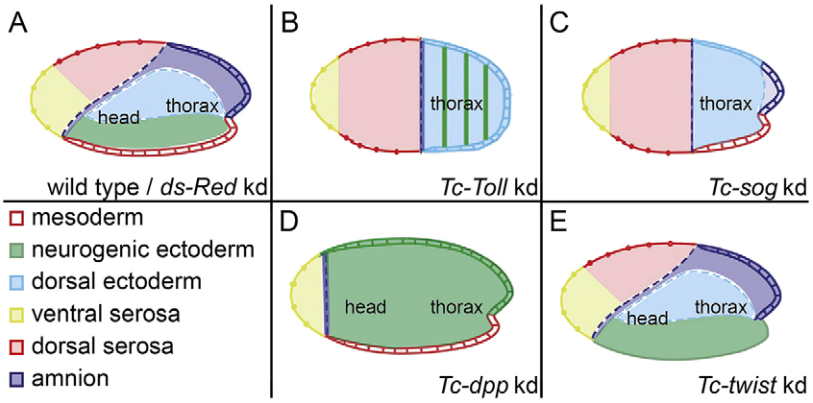

Fig. 1. Schematic representation of dorsoventral phenotypes. Fate maps of wild-type (A), *Tc-Toll* knockdown (B), *Tc-sog* knockdown (C), *Tc-dpp* knockdown (D) and *Tc-twist* knockdown (E) *Tribolium* embryos at the beginning of gastrulation (Fonseca et al., 2009).

Development (2016) 143, 2443-2454 doi:10.1242/dev.130641

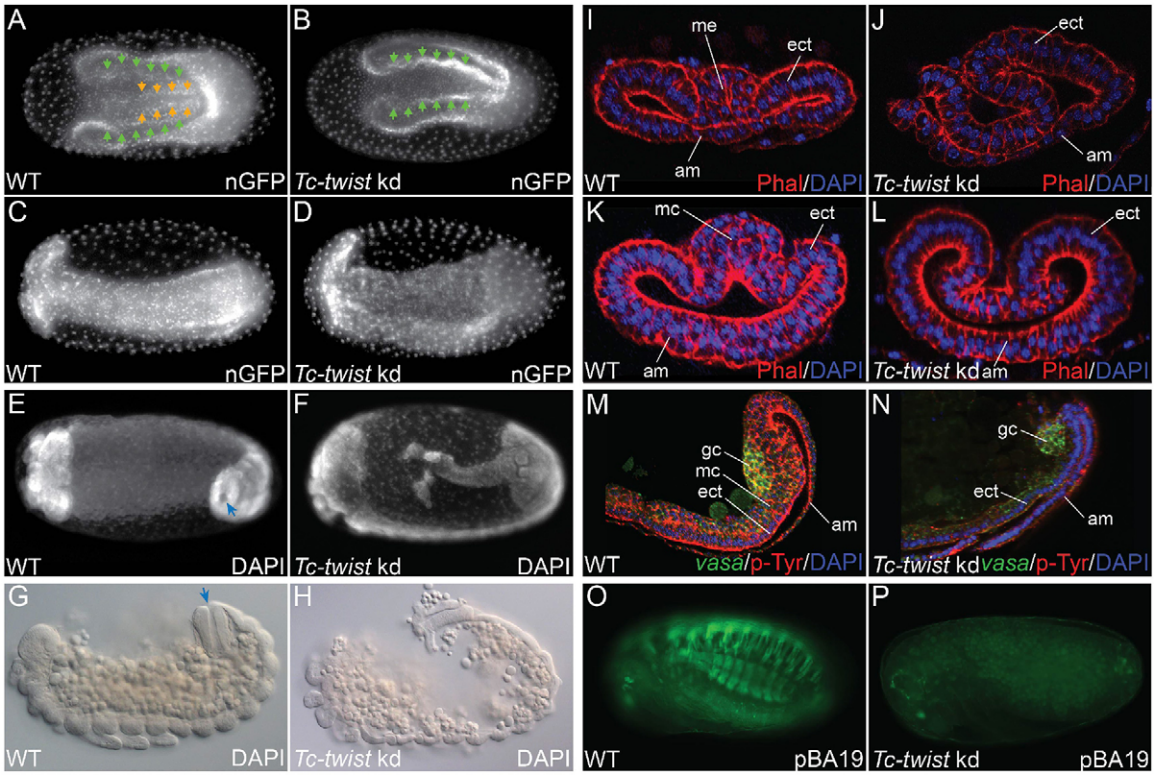

Fig. 2. *Tc-twist* is required for ventral furrow formation and mesoderm specification. (A-D) Stills from movies of an nGFP line (see Movies 1-3). (A,B) Embryos at horseshoe stage of amniotic fold formation (Benton et al., 2013). Condensation of the germ band is indicated by green arrows. (A) In the wild type (WT), the rim of the ventral furrow is marked by orange arrowheads. In the *Tc-twist* knockdown (B), ventral furrow formation is lacking. (C,D) Embryos at extending germ band stage. The *Tc-twist* knockdown embryo (D) is less compact and the lateral extension of the germ band is wider than that of the wild-type embryo (C). (E,F) Dorsal views of DAPI-stained retracting germ band embryos. (E) Wild-type embryo shows the opening of the invaginated hindgut (blue arrow). (F) In the *Tc-twist* knockdown, the hindgut is detached from its normal position and points posteriorly with Malpighian tubules visible at its tip. (G,H) Lateral views of retracting germ band embryos (Nomarski optics). In the wild type (G), the opening of the hindgut is at the posterior end of the embryo (blue arrow), whereas in the *Tc-twist* knockdown (H), the hindgut points posteriorly and the Malpighian tubules protrude at its anterior end. (I-L) Cross sections through the anterior (I,J) and posterior (K,L) trunk region of gastrulating embryos stained with DAPI (blue) and Phalloidin (red). In the wild type (I,K), the mesodermal cells invaginate along the ventral midline (ventral furrow) and lose their epithelial organization; in *Tc-twist* knockdown (J,L), ventral furrow formation is lacking. (M,N) Sagittal sections through posterior region (including the growth zone) of extending germ band embryos stained with DAPI (blue), anti-phospho-tyrosine (red) and *Tc-vasa* ISH (green). In the wild type (M), the growth zone is covered by the amnion (am) and has three cell layers: the germ cells (gc) stained for Vasa (green), the mesenchymal layer (mc) and the ectodermal layer (ect). In the *Tc-Twist* knockdown (N), the mesenchymal layer is missing and the germ cells (green) rest on the ectodermal layer. (O,P) Embryos of the pBA19 enhancer trap line embryo. (O) EGFP expression in somatic muscles of the wild type. (P) *Tc-Twist* knockdown embryo lacks EGFP expression in somatic muscles.

zone during later developmental stages. Based on this data we suggest that, as in *Drosophila*, knockdown of *twi* in *Tribolium* leads to the absence of most, if not all mesodermal derivatives during later development. However, while *Drosophila twi* mutants have a twisted germ band, leading to a highly abnormal cuticle phenotype (Simpson, 1983), the loss of mesodermal derivatives has no detectable consequences for ectodermal development in *Tribolium*. *Tc-twi* RNAi embryos show largely normal germ band extension (Fig. 2H) and retraction (Fig. S2B). In addition, extraembryonic development, including dorsal closure, occurs as in the wild type, and the secreted cuticles lack overt defects (Fig. S2C,D).

Identification of DV patterning genes by transcriptome analysis

We knocked down *Tc-Toll*, *Tc-twi*, *Tc-dpp* and *Tc-sog* by pRNAi and subsequently sequenced the transcriptomes of the respective knockdown embryos. We then compared the transcriptomes of knockdown and control embryos to identify genes that are regulated by *Tc-Toll*, *Tc-twi* or by BMP signalling. As a control, the transcriptomes of offspring laid by mothers injected with dsRNA specific for *dsRed* were sequenced. *dsRed* is not encoded in the *Tribolium* genome and should not specifically affect gene expression, but this treatment accounts for possible expression changes caused by injection of dsRNA. To investigate if there are such unspecific expression changes we also sequenced the transcriptomes of embryos derived from untreated wild-type mothers.

After verification of the general knockdown penetrance in embryos laid by injected mothers (>90% for each treatment, data not shown), RNA was prepared from narrowly staged embryos (7.5 h to 11.5 h after egg laying at 30°C), which ranged in age from undifferentiated blastoderm to early gastrulation (horseshoe amniotic fold stage; Benton et al., 2013). The knockdown efficiency (~60-70%) in each individual RNA sample was verified by qRT-PCR (Fig. S1). Finally, 24 samples were chosen for sequencing: five biological replicates each for *Tc-Toll* knockdown, *Tc-twi* knockdown and wild-type embryos and three biological replicates each for *Tc-sog*, *Tc-dpp* and *dsRed* knockdown embryos. The data were processed (see Material and Methods) and tested for differentially expressed genes using two independent

Development (2016) 143, 2443-2454 doi:10.1242/dev.130641

algorithms. Only genes that were detected to be differentially expressed by both algorithms were further considered. Interestingly, no genes were differentially expressed between untreated embryos and embryos from mothers injected with *dsRed* [false discovery rate (FDR) of 5%]. This is an important result in itself, as it indicates that gene expression is only affected by pRNAi against endogenous genes and shows that untreated embryos are a sufficient control in future experiments. To gain additional statistical power for analysis of the knockdown transcriptomes, transcriptomes from both *dsRed* pRNAi and wild-type embryos were treated as controls.

Comprehensive analysis identifies more than 750 differentially expressed genes

In total, 796 genes were differentially expressed with a FDR of 1% compared with control embryos (Fig. 3A): 347 upon *Tc-twi*, 310 upon *Tc-Toll*, 18 upon *Tc-sog* and 377 upon *Tc-dpp* knockdown (Tables S1-S5). To narrow down the large numbers of differentially expressed genes, we focused on those 222 genes that were differentially expressed in more than one knockdown situation (Fig. 3A; Table S6). As expected, the genes regulated by dorsalizing and ventralizing genes were predominantly regulated in opposite directions (e.g. *dpp* and *Toll*). Genes co-regulated by two ventralizing genes were mostly regulated in the same direction (e.g. *Toll* and *twist*) (Fig. 1 and Fig. 3B).

Fate shift of knockdown embryos is predictive for the expression domain of differentially expressed genes

To find genes that act in the neuroectoderm or dorsal ectoderm, we focused on comparison of *Tc-dpp* and *Tc-sog* knockdown. As described earlier, *Tc-dpp* knockdown leads to a massive expansion of neuroectoderm, while *Tc-sog* knockdown results in the opposite phenotype, that being an almost complete loss of the neuroectoderm. Both knockdowns have little impact on the mesoderm (Fig. 1). We found 14 genes to be differentially expressed in these opposing situations at an FDR of 1% (Fig. 3A; Table S7). Of these, 10 genes are downregulated upon *Tc-dpp* knockdown and upregulated upon *Tc-sog* knockdown (Fig. 3B; Table S7) and the remaining 4 genes show the reverse behaviour (Fig. 3B). As predicted from the fate map shifts (Fig. 1), genes belonging to the former group are mainly, and often exclusively, expressed in the serosa (Fig. 4A-E, data not shown for TC006222, TC010855, TC001439 and TC015188; TC008855 could not be cloned), while genes belonging to the latter group are expressed in the neurogenic ectoderm (Fig. 4F-H). The neuronal cell fate determinant *TC010596*/*Tc-prospero* (Fig. 4H and data not shown) (Biffar and Stollewerk, 2014; Ungerer et al., 2011) and the leucine-rich repeat (LRR) transmembrane protein *TC014658*/*Tc-tartan* (Fig. 4G and Fig. 5F) (Chang et al., 1993) both show broad neuroectodermal expression along the entire AP axis. In addition, *TC014658*/*Tc-tartan* is upregulated in a wedge-shaped region of the head anlage. The other two genes, *TC004745*/*Tc-patched* (Fig. 4F) (Farzana and Brown, 2008) and *TC007409*/*Tc-twin of eyeless* (data not shown, see Yang et al., 2009), show high expression in the head region of differentiated blastoderm embryos. This region is lost upon dorsalization and expanded upon ventralization (Fig. 1). To search the dataset for more candidates we also included some genes selected with a FDR of 5% (Table S7), e.g. *TC000871*/*Tc-uninflatable* (*Tc-uif*), which is known to be involved in Notch signalling in *Drosophila* (Xie et al., 2012; Zhang and Ward, 2009).

Functional analysis of neuroectodermal and serosal genes

We next functionally tested three of the identified genes: *Tc-uif*, *Tc-tartan* and one of the genes expressed in the serosa, *TC006771*. For each knockdown, we analysed survival of the injected mothers, the

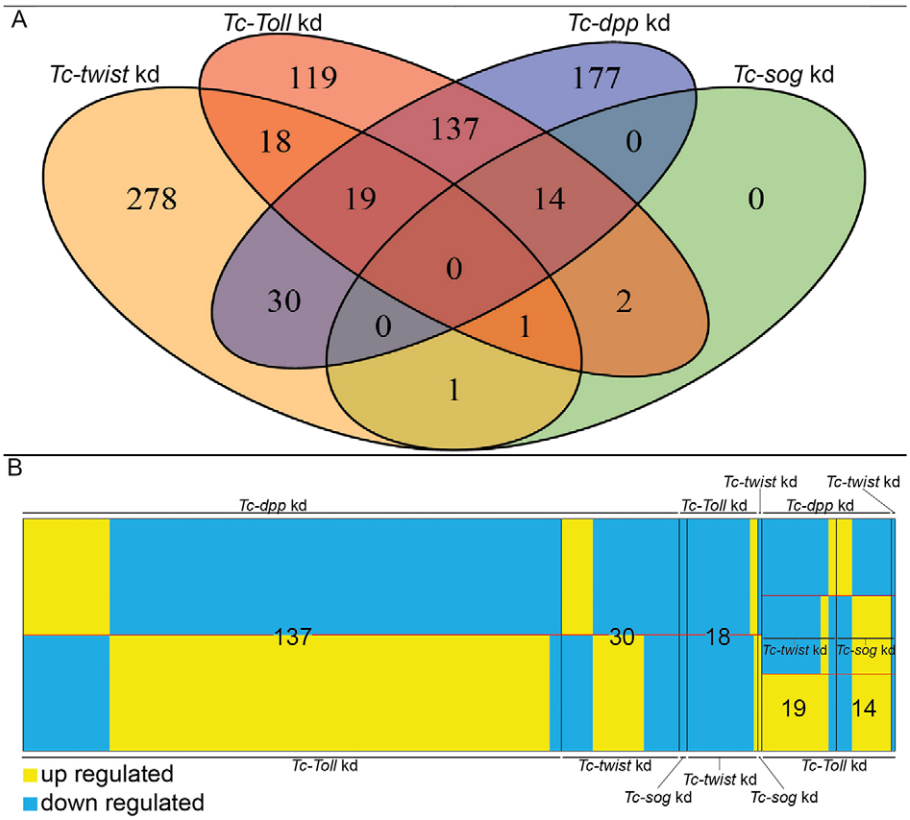

Fig. 3. A total of 222 genes are differentially expressed in more than one knockdown condition. (A) Venn diagram depicting the number of genes that are differentially expressed upon knockdown of *Tc-twist*, *Tc-Toll*, *Tc-dpp*, *Tc-sog* compared with wild-type embryos. Each field in the Venn diagram shows the number of genes that are exclusively found in the overlap of conditions indicated by the diagram. For the identity of corresponding genes, see Table S6. (B) Heat map showing if genes that are found in the overlapping fields of the Venn diagram are upregulated (yellow) or downregulated (blue). The numbers in the figure correspond to the numbers in the fields of the Venn diagram.

Development (2016) 143, 2443-2454 doi:10.1242/dev.130641

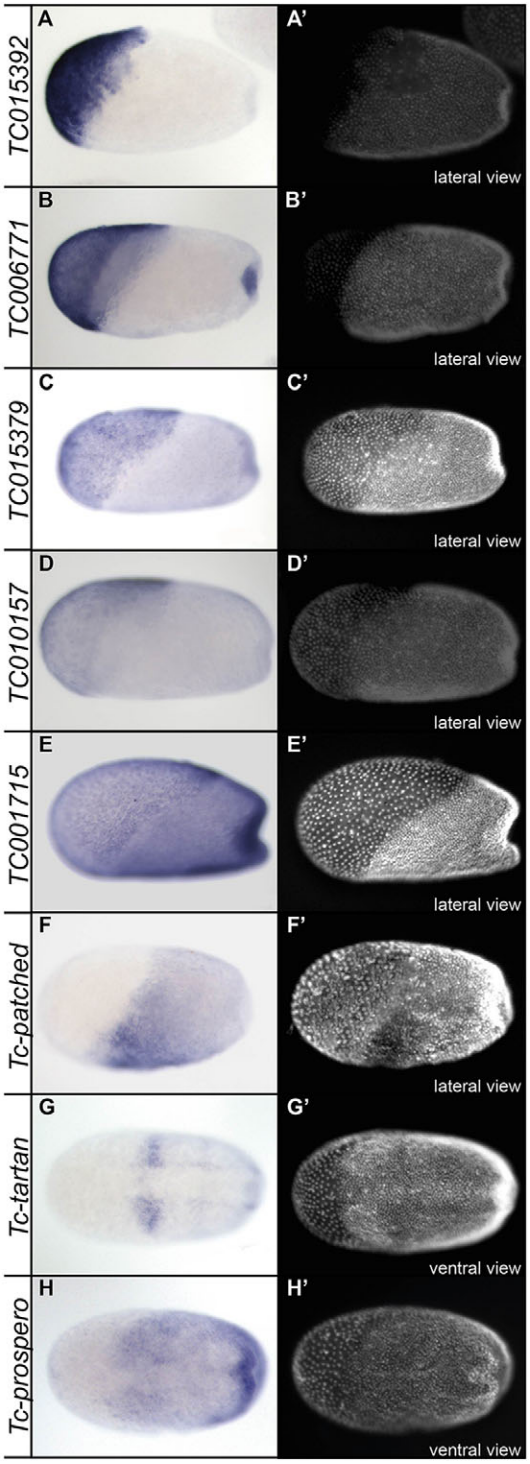

Fig. 4. Expression patterns of genes differentially regulated upon knockdown of *Tc-sog* and *Tc-dpp*. (A-H) Whole-mount ISH of embryos at the primitive pit stage (A-D) or early gastrulation stage (E-H). (A′-H′) DAPI staining of the respective embryos. The anterior pole points to the left, the dorsal side points upwards, except for G,H, which show ventral surface views. (A-D) Expression in the serosa. Note that *TC015392* is just expressed in part of the serosa and that *TC006771* is also expressed in the primitive pit. (E) *TC01715* is expressed in the serosa, but also in the germ rudiment. (F-H) Expression in the germ rudiment. *Tc-patched* shows stronger expression in the presumptive head region (F). *Tc-tartan* is upregulated in a stripe within the presumptive head region (G) and expression is absent from the mesoderm. *Tc-prospero* is expressed uniformly in the presumptive neuroectoderm and downregulated in the mesoderm (H).

morphology of DAPI-stained embryos and the expression of marker genes for DV cell specification: *Tc-pannier* (*Tc-pnr*, amnion; van der Zee et al., 2005), *Tc-twi* (mesoderm) and *Tc-achaete-scute homolog* (*Tc-ash*, neuronal precursors; Wheeler et al., 2003). *Tc-engrailed* (*Tc-en*) and/or *Tc-gooseberry* (*Tc-gsb*) (Brown et al., 1994; Davis et al., 2001; Nunes da Fonseca et al., 2008) (Fig. S3) were used to monitor segmentation.

Tc-uif is first expressed in the neurogenic ectoderm with increasing expression levels towards the border of the presumptive mesoderm (Fig. 5A,B). Later, *Tc-uif* is expressed in the whole germ band with the exception of the mesoderm (Fig. 5C). *Tc-uif* knockdown leads to embryos with thinner and twisted abdomens (61.45%, n=182) (Fig. 5D,E). However, none of the marker genes used to analyse the phenotype showed altered expression patterns in early embryos (Fig. S3). Thus, despite the early expression of *Tc-uif*, the phenotype apparently arises during later development within the growth zone.

Early neuroectodermal and head expression of *Tc-tartan* (Fig. 4G and Fig. 5F) is followed by segmental expression in later stages (Fig. 5G,H). *Tc-tartan* is not expressed in the mesoderm; however, upon knockdown of *Tc-twi* (Fig. 5I, compare with Fig. 4G), its expression expands into the future mesoderm, suggesting a suppressive function of *Tc-twi* or of a *Tc*-Twi target gene. Expression analysis of *Tc-ash* shows that *Tc-tartan* is involved in neurogenesis because cells expressing *Tc-ash* (marking proneural clusters) were largely lost upon knockdown of *Tc-tartan* (Fig. 5J,K).

Upon *TC006771* knockdown, we observed embryos with interrupted germ bands and thin abdominal segments. However, the penetrance of this phenotype was low (6.86% of all embryos, n=322). Although comparable defects are not seen in controls, we did not further investigate this phenotype. Taken together, by comparing the transcriptomes of severely ventralized embryos with that of severely dorsalized embryos, we identified new genes expressed in the serosa and discovered new early functions for genes that are only required at later stages in *Drosophila* (see Discussion). In particular, *Tc-tartan* appears to be a component of the *Tribolium* DV-GRN required for early neurogenesis.

Ventrally expressed genes are detected by analysing *Tc-Toll* and *Tc-twi* knockdown embryos

While *Tc-Toll* knockdown results in a strong dorsalization, *Tc-twi* knockdown has only minor effects on the early fate map (Fig. 1). Furthermore, *Tc-twi* is downstream of *Tc-Toll* (Nunes da Fonseca et al., 2008). Therefore, we hoped to identify more direct targets of the early DV-GRN by focusing on the group of genes that are downregulated upon knockdown of both *Tc-Toll* and *Tc-twi*. This assumption is supported by the observation that both *Tc-twi* and *Tc-cactus* (which is dependent on *Tc-Toll* and *Tc-twi*) are among the 19 genes that fall into this category with an FDR of 1%. (Nunes da Fonseca et al., 2008) (Table S8; Fig. 6A,B). Further, *Tc-snail* seems to be regulated by *Tc-Toll* and *Tc-twi* (Fig. 6C), like in *Drosophila* (Reeves and Stathopoulos, 2009). The same applies for the homologues of the *Drosophila twi* target genes *heartless* (*htl*) and *down of FGF receptor* (*dof*) (Beermann and Schröder, 2008; Beiman et al., 1996; Gisselbrecht et al., 1996; Imam et al., 1999; Vincent et al., 1998) (Fig. 6D,E). Interestingly, *Tc-Delta* expression depends on *Tc-Toll* and *Tc-twi* and is found in the presumptive mesoderm in wild-type embryos (Fig. 6F). This is strikingly different from *Drosophila*, where *Delta* is repressed in the presumptive mesoderm and shows graded expression in the neurogenic ectoderm (Vassin et al., 1987). Along with *Tc-Delta*,

Development (2016) 143, 2443-2454 doi:10.1242/dev.130641

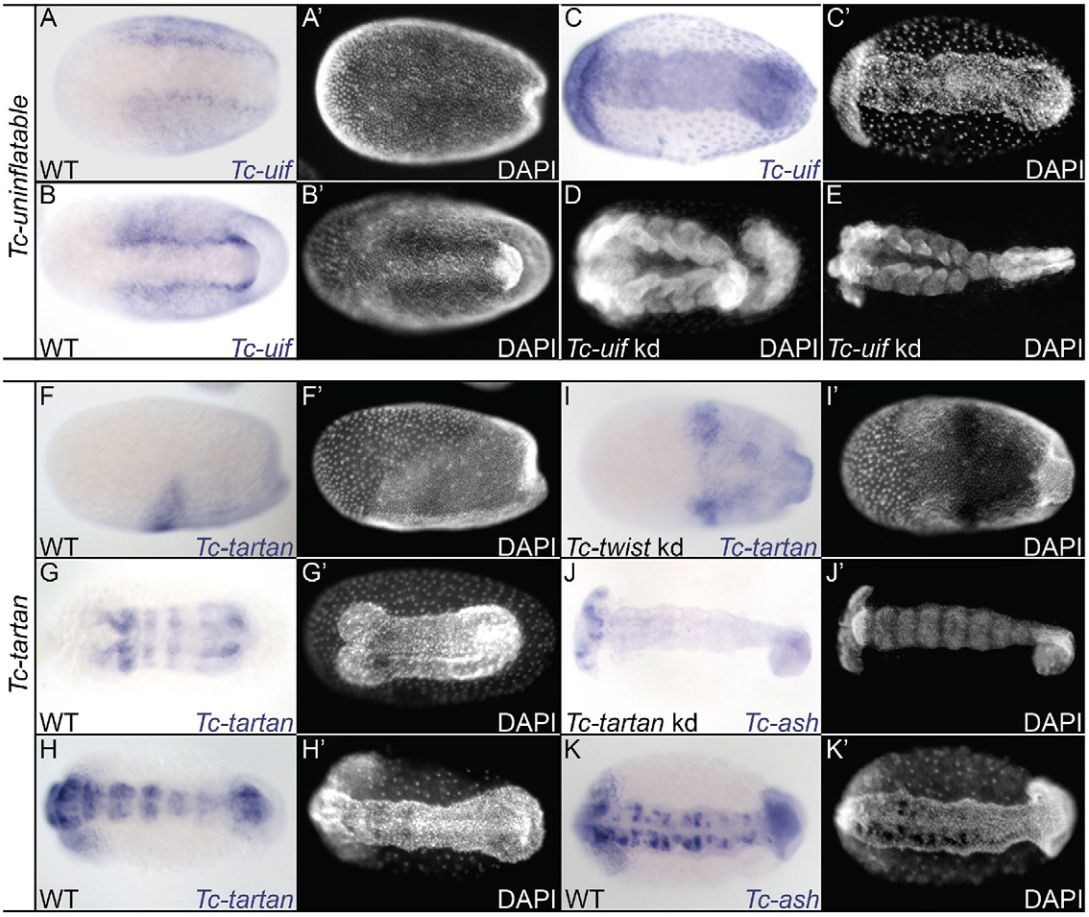

Fig. 5. *Tc-uninflatable* and *Tc-tartan* are required for embryogenesis. (A-C,F-K) Whole-mount ISH. (A′-C′,F′-K′) DAPI staining of the respective embryos. Ventral surface views, except for F, which shows a lateral view. Anterior points to the left. (A-C) Expression of *Tc-uninflatable* (*Tc-uif*) in wild-type embryos. (A,B) *Tc-uif* is expressed in the ectoderm with increased levels towards the mesodermal border at primitive pit stage (A) and early gastrulation (B). (C) *Tc-uif* expression is maintained in the ectoderm during germ band extension. (D,E) *Tc-uif* knockdown. DAPI staining of embryos during germ band extension (~24-48 h after egg laying). The abdominal segments of *Tc-uif* knockdown embryos are thinner and often bent. (F-H) Wild-type expression of *Tc-tartan*. High expression levels of *Tc-tartan* are seen in the head anlagen and weak expression in the neuroectoderm at early gastrulation (F). Neuroectodermal expression of *Tc-tartan* becomes segmental during germ band extension (G,H). (I) Upon knockdown of *Tc-twist*, the neuroectodermal expression of *Tc-tartan* expands towards the ventral side. (J) *Tc-tartan* knockdown results in loss of the neuroblast precursor cells, indicated by the absence of *Tc-achaete-scute (Tc-ash)*-expressing cells compared with the wild type (K).

the two enhancer of split homologues of *Tribolium Tc-E(spl)1* and *Tc-E(spl)3* (Kux et al., 2013) are regulated by *Tc-Toll* and *Tc-twi* and are expressed in a mesodermal domain with higher levels toward the lateral borders (Fig. 6G,H). Expression of *E(spl)* complex genes within the presumptive mesoderm has also not been reported for *Drosophila* (Knust et al., 1992; Wech et al., 1999).

The genes *TC001667*/*integrin αPS2 (inflated)*, *TC005328*, *TC010105*/*l(2)efl* and *TC010461* were also downregulated upon *Tc-twi* and *Tc-Toll* knockdown, and are weakly expressed in the mesoderm of wild-type embryos (Fig. 6I-L). The remaining genes from this group (*TC003461*, *TC003606*, *TC007056*, *TC009862*, *TC010195*, *TC013142*) were cloned, but did not show a specific expression pattern, with the exception of the pair-rule gene *TC008064*/*Tc-sloppy paired* (Choe and Brown, 2007), which is expressed in stripes along the anterior-posterior axis (Fig. 6M).

In summary, most of the genes that are downregulated upon knockdown of *Tc-twi* and *Tc-Toll* are expressed in the presumptive mesoderm shortly before gastrulation. Given their early expression pattern they might be directly regulated by both *Tc-Toll* and *Tc-twist*, or by *Tc-twist* alone.

Functional analysis of ventrally expressed genes

For functional analysis, we chose *TC004713*/*Tc-htl*, the sole FGF receptor of *Tribolium* and *TC011323*/*Tc-dof*, a cytoplasmic signal transducer downstream of the FGF receptor (Fig. S4), as well as two genes selected with reduced stringency (5% FDR): *TC011114*/*Tc-zinc-finger homeodomain 1* (*Tc-zfh1*) and *TC005184*/*Tc-LamininB1* (*Tc-LanB1*, Fig. S4). All four genes are expressed in the presumptive mesoderm at the primitive pit stage (Fig. 6D,E and Fig. 7E,K).

Knockdown of *Tc-htl* or *Tc-dof* does not affect expression of the aforementioned marker genes suggesting no major patterning defects during germ band extension (Fig. S4A-M). However, using the transgenic line G04609 (Koelzer et al., 2014), we observed that knockdown of *Tc-htl* resulted in complete loss of cardioblasts (Fig. 7A,B) confirming earlier observations (Sharma et al., 2015), whereas *Tc-dof* knockdown resulted in a partial loss of this tissue (Fig. 7A,C). In addition, *Tc-htl* embryos show a mispositioned hindgut with Malpighian tubules protruding at the tip, as in *Tc-twi* knockdown embryos (compare Fig. 7B with Fig. 2F and Fig. S2B,D; see also Sharma et al., 2015). This hindgut phenotype was, however, never observed in *Tc-dof* knockdown

Development (2016) 143, 2443-2454 doi:10.1242/dev.130641

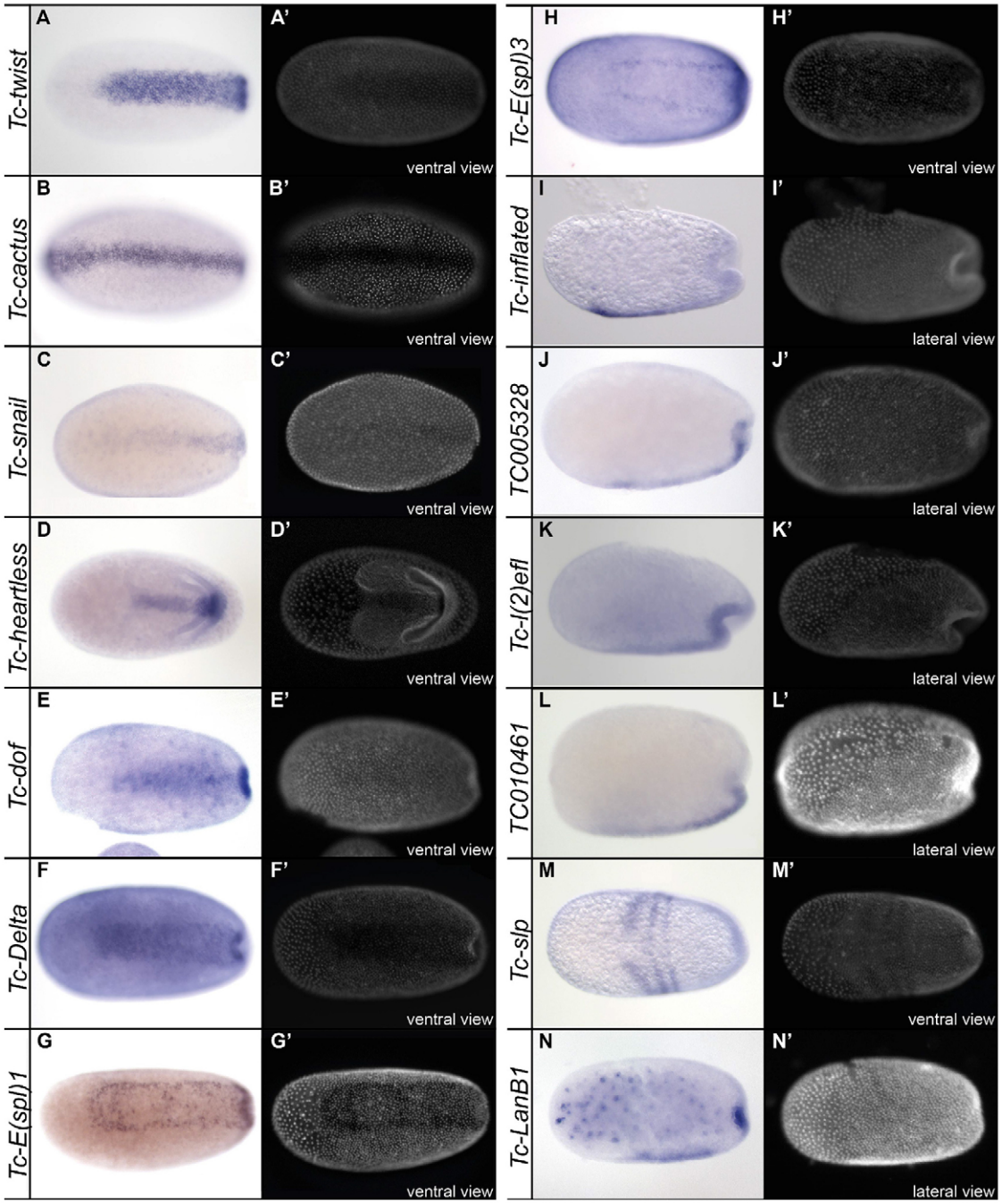

Fig. 6. Expression of genes differentially regulated upon knockdown of *Tc-Toll* and *Tc-twist*. (A-N) Whole-mount ISH of embryos at blastoderm stage (A-C), primitive pit stage (E-H,J,L,M,N) or early gastrulation stage (D,I,K). (A′-N′) DAPI staining of the respective embryos. The anterior pole points to the left. (A-H,M) Ventral surface views. (I-L,N) Lateral views with dorsal side pointing upwards. All genes (except in G,H and M) are expressed in the presumptive mesoderm. Note that *Tc-cactus* (B) is also expressed in ventral parts of the serosa. *Tc-E(spl)1* (G) and *Tc-E(spl)3* (H) are expressed in narrow lateral stripes at the border of the mesoderm.

embryos (Fig. 7C,D). In the course of a genome-wide RNAi screen in *Tribolium*, the impact on somatic muscle differentiation was also significantly weaker for knockdown of *Tc-dof* than *Tc-htl* (Donitz et al., 2015; Schmitt-Engel et al., 2015). This indicates that *Tc-dof* is not required for all aspects of FGF signalling in *Tribolium*, which is in contrast to *Drosophila* where *dof* mutants almost completely abolish FGF signalling (Imam et al., 1999; Vincent et al., 1998). The fact that *Tc-htl* and *Tc-twi* knockdown cause the same hindgut phenotype suggests that *Tc-twi* primarily acts via FGF signalling to control hindgut morphogenesis.

Tc-zfh1 expression is maintained in the mesoderm during gastrulation and germ band extension (Fig. 7F,G). Knockdown of *Tc-zfh1* results in reduced survival of injected adult beetles (28% survival, n=200; compared with *Tc-Toll* and *Tc-twist* injected beetles with 72% and 78% survival, respectively, n=300) and reduced egg production. Reduction of the dsRNA from 1 µg/µl to 0.1 µg/µl alleviated the sterility effect and allowed expression analysis of marker genes (Fig. S4N-Q). Interestingly, of the four investigated marker genes, only *Tc-twi* expression was affected. Although early *Tc-twi* expression is normal upon knockdown of

Development (2016) 143, 2443-2454 doi:10.1242/dev.130641

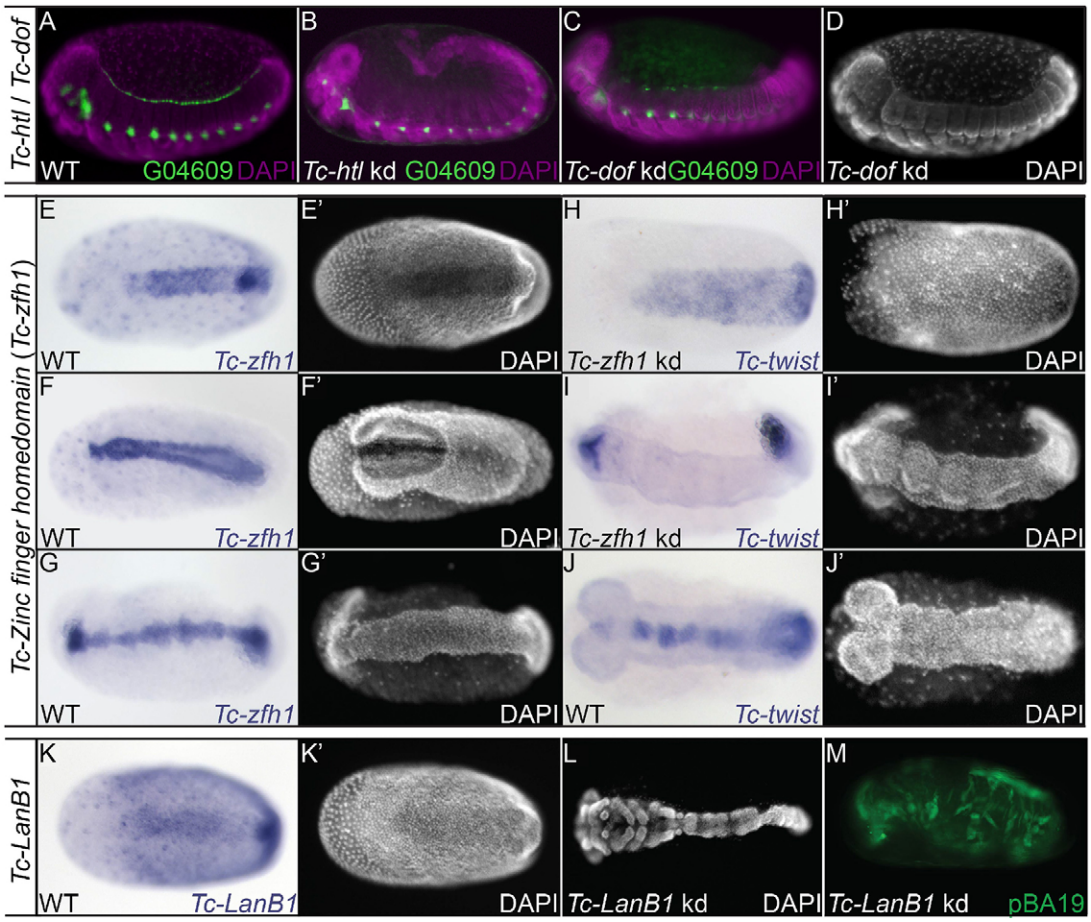

Fig. 7. Functional analysis of mesodermally expressed genes. (A-D) Lateral views of embryos after germ band retraction. Enhancer trap line G04609 results are shown in A-C. (A) Wild-type embryo showing GFP expression in cardioblasts and unspecified clusters of lateral cells (Fig. S2). (B) *Tc-htl* knockdown leads to loss of cardioblast and to a protruding hindgut. (C) *Tc-dof* knockdown leads to a reduced number of cardioblasts. The hindgut is not protruding. (D) DAPI-stained *Tc-dof* knockdown embryo after germ band retraction. The hindgut is protruding. (E-K′) Ventral surface views of embryos after whole-mount ISH (E-K) and DAPI staining (E′-K′). Wild-type expression of *Tc-zfh1* is shown in E-G. (E) Differentiated blastoderm. *Tc-zfh1* is expressed in the presumptive mesoderm. (F) Gastrulation. (G) Germ band extension. *Tc-zfh1* is expressed in the mesoderm. *Tc-twist* expression is shown in H-J. (H) *Tc-zfh1* knockdown. Early *Tc-twist* expression is not affected. (I) *Tc-zfh1* knockdown. *Tc-twi* expression is missing in thoracic and abdominal segments of germ-band stage embryos, compared with *Tc-twist* in the wild type (J). (K) *Tc-LanB1* is expressed in the whole germ rudiment and upregulated in the presumptive mesoderm in differentiated blastoderm embryos. (L) *Tc-LanB1* knockdown. DAPI-stained germ-band stage embryo shows defects in posterior segments. (M) *Tc-LanB1* knockdown in pBA19, which shows GFP expression in somatic muscles. The somatic muscles are partially lost and severely disorganized (see also Fig. S5).

Tc-zfh1, *Tc-twi* is lost in abdominal segments during germ band extension (Fig. 7, compare I with J). This suggests that *Tc-zfh1* is required to maintain *Tc-twi* expression subsequent to the activation of *Tc-zfh1* by *Tc-twi*. In *Drosophila*, mutations of *zfh1* only cause weak muscle phenotypes (see Discussion) (Lai et al., 1993).

Tc-LanB1 is expressed in the entire germ rudiment and upregulated in the presumptive mesoderm (Fig. 6N and Fig. 7K). *Tc-LanB1* knockdown embryos show no early embryonic defects based on the selected marker genes (Fig. S4R-U). However, the abdomen of extended germ band embryos is thinner and irregularly shaped. *Tc-LanB1* knockdown in the muscle enhancer line pBA19 reveals a broad spectrum of muscle defects ranging from mild disorganization to complete loss of body wall muscles (Fig. 7M and Fig. S5A-D), whereas cardioblasts are always lost (Fig. S5E-H). In *Drosophila*, the complete loss of LanB1 function leads to much milder defects during late organogenesis (Urbano et al., 2009).

Taken together, selecting genes that were downregulated after *Tc-Toll* and *Tc-twi* RNAi led to the discovery of new expression patterns, such as the mesodermal expression of the *Tc-E(spl)* genes, as well as new early phenotypes caused by the knockdown of genes known to have later roles in *Drosophila*. In particular, *Tc-zfh1* is likely to be a component of the *Tribolium* DV-GRN that is required to maintain the expression of *Tc-twi*, the key regulator of mesoderm development.

DISCUSSION

To understand the *Tribolium* DV-GRN it is necessary to identify all of its components, irrespective of homologues in other species. By knocking down key regulators of DV patterning followed by comprehensive transcriptome analysis, we identified over 750 differentially expressed genes. This dataset is a valuable resource, not only for the identification of early, locally expressed genes, but also for the unbiased identification of DV network components. In this study, we focused only on those genes that were differentially expressed in more than one knockdown situation. Even this resulted in a number (222) that precluded complete and careful analysis. We therefore selected two subgroups for in-depth study: the 14 genes differentially expressed between *Tc-dpp*, *Tc-sog* and *Tc-Toll* knockdowns and the 19 genes downregulated upon *Tc-*

Development (2016) 143, 2443-2454 doi:10.1242/dev.130641

Toll and *Tc-twi* knockdown. We expected to identify ectodermal genes in the first group and mesodermal genes in the second group. Five genes from the first group show expression only in the (anterior-dorsal) serosa and three are upregulated in the (anterior-ventral) head region. This high number of genes with differential expression along the AP axis reflects the aforementioned fact that the sizes of the serosa and head anlagen are affected by global DV patterning genes like *Tc-Toll*, *Tc-sog* and *Tc-dpp*. In contrast, the second group requiring downregulation following *Tc-twi* knockdown did not result in the selection of AP patterning genes, and thus is more likely to be enriched in bona fide elements of the DV-GRN. However, further experiments such as ChIP-seq or detailed molecular studies will be necessary to understand the regulatory wiring connecting these genes. From our data, we chose a limited number of genes for functional analysis by RNAi. In the following, we will first discuss the *Tc-twi* knockdown phenotype before returning to the genes identified through comparative transcriptome analysis.

Similarities and differences of *twi* function in *Tribolium* and *Drosophila*

Live imaging of knockdown embryos in enhancer trap lines demonstrated that *Tc-twi* function is largely confined to the mesoderm and that the loss of the mesoderm has little effect on the rest of the embryo. With the exception of ventral furrow formation, all early (folding of the amnion, germ band extension) and most of the late morphogenetic movements (germ band retraction, opening of the amniotic cavity and dorsal closure) are not obviously affected (Fig. 2; Fig. S2A,B). Only the hindgut is not positioned correctly. The *Tc-twi* knockdown embryos secrete a cuticle that is hard to distinguish from controls (Fig. S2C,D). However, *Tc-twi* knockdown larvae completely lack somatic mesoderm as well as cardioblasts. Thus, in *Tribolium*, ectodermal development occurs apparently largely independent of mesodermal specification. This phenotype is remarkable as the *Drosophila twi* mutants have been identified by virtue of their strong cuticular defects, which include head defects, incomplete germ band retraction and an overall twisted appearance (Simpson, 1983).

The *Tc-twi* knockdown phenotype also provides interesting insights into mesoderm formation in the growth zone. In an earlier study, it was suggested that the inner mesenchymal cell layer of the growth zone is derived from cells that had been internalized through ventral furrow formation in the early embryo, which maintain a mesodermal identity and later give rise to the mesoderm of the newly forming segments (Handel et al., 2005). However, the lack of *Tc-twi* expression in these inner layer cells represented a caveat for this hypothesis, because in *Drosophila*, mesodermal precursor cells continue to express *twi*. The *Tc-twi* knockdown phenotype resolves this problem, as the growth zone of the knockdown embryos lack the inner mesenchymal cell layer. Thus, these cells indeed are derived from cells internalized through prior ventral furrow formation – the process that is blocked upon *Tc-twi* knockdown.

The hindgut phenotype of *Tc-twi* knockdown represents an interesting deviation from *Drosophila*. After *Tc-twi* knockdown, the hindgut does not point to the interior of the embryo where it is usually connected to the midgut, but it rather points posteriorly and the Malphigian tubules form finger-like protrusions at its tip (Fig. 2E-H). We observed a virtually identical phenotype after knockdown of *Tc-htl* (Fig. 7B). *Tc-htl* knockdown embryos lack *Tc-twi*-expressing cells surrounding the hindgut and are likely to give rise to the caudal visceral mesoderm (CVM) (King and Denholm, 2014; Sharma et al., 2015). Thus, in *Tribolium*, *Tc-twi* appears to be required for the formation of the CVM and this effect is probably not only indirect through regulation of FGF signalling by *Tc-twi*, but also direct since the CVM precursor cells express *Tc-twi*. In contrast, in *Drosophila*, the CVM cells do not express *twi* and represent the only group of mesodermal cells that can form in the absence of *twi* (Kusch and Reuter, 1999). This observation indicates that the extent to which *twi* was recruited to specify different mesodermal subtypes varies between insect lineages.

Stronger knockdown phenotypes for orthologues in *Tribolium* compared with *Drosophila*

Among the ectodermally expressed genes, *Tc-uif* and *Tc-tartan* showed interesting early expression patterns and were selected for functional analysis. In *Drosophila*, *uif* is required during late embryogenesis (tracheal inflation; Zhang and Ward, 2009) and during imaginal disc development where it acts as a Notch antagonist (Loubéry et al., 2014; Xie et al., 2012). No early developmental functions of *uif* have been discovered, although the expression of *Drosophila uif* already starts before gastrulation in a pattern reminiscent to that of *Tc-uif* (Zhang and Ward, 2009). In *Tribolium*, *uif* is clearly required for embryonic development because *Tc-uif* knockdown affects growth zone patterning or morphogenesis.

Tartan and its close homologue Capricious are transmembrane proteins with extracellular leucine-rich repeats (LRRs). In *Drosophila*, *tartan* is first expressed in a double-segmental (pair-rule like) pattern and later in proneural clusters and sensory mother cells (Chang et al., 1993). For *capricious*, only late embryonic expression in motorneurons and muscles was reported. In *Tribolium*, we identified only one gene with similarity to both *tartan* and *capricious*. Since this *Tribolium* gene shares some aspects of early embryonic expression with *Drosophila tartan*, we named it *Tc-tartan* (Fig. 5G-H). Loss of *tartan* in *Drosophila* leads to weak defects during late peripheral and central nervous system development (Chang et al., 1993). As there is no information on the embryonic phenotype of the double mutant between *tartan* and *capricious* we cannot exclude that deletion of both genes has a more severe embryonic phenotype in *Drosophila*. In wing imaginal discs, both genes act together to stabilize the DV compartment boundary (Milán et al., 2005, 2001). However, the lack of a prominent early embryonic expression of *capricious* does not support a similar interaction for the early *Drosophila* embryo. In *Tribolium*, loss of *Tc-tartan* leads to a severe and interesting phenotype: the absence of proneural clusters marked by *Tc-ash* expression (Fig. 5J). This indicates that *tartan* has an essential function in early CNS development in *Tribolium*. Thus, as in the case of *Tc-uif*, the *Tc-tartan* phenotype appears to be substantially stronger than that of the corresponding *Drosophila* gene.

As *Tc-twist* knockdown only affects the mesoderm, the expression of genes that are downregulated upon both *Tc-Toll* and *Tc-twist* knockdown should be restricted to the mesoderm. This prediction was confirmed: from 19 genes selected with an FDR of 1%, 12 showed mesodermal expression. By relaxing the FDR to 5%, additional ventrally expressed genes were identified. Besides known candidates (*Tc-twi*, *Tc-snail*, *Tc-cactus*), representatives of two signalling pathways (Notch and FGF) and components involved in cell adhesion (integrins, laminin and dystroglycan) were identified (Table S8). Only one of the newly identified genes, *Tc-zfh-1*, encodes a transcription factor.

While expression and function of the FGF pathway components *Tc-htl* (the single FGF receptor) and *Tc-dof* (an

Development (2016) 143, 2443-2454 doi:10.1242/dev.130641

adaptor protein) is very similar to that of the *Drosophila* homologues (Beermann and Schröder, 2008; Sharma et al., 2015), the expression of Notch pathway components deviates strikingly. In particular the broad ventral expression of the Notch ligand *Delta* (Aranda et al., 2008) and the two *Tribolium E(spl)* homologues suggest that Notch signalling is active in the presumptive mesoderm. In *Drosophila*, Notch signalling is inhibited in the mesoderm through several parallel mechanisms, including the repression of Delta (Bardin and Schweisguth, 2006; De Renzis et al., 2006; Vassin et al., 1987).

The early mesodermal expression of the extracellular matrix receptor αPS2 integrin (*inflated*) is shared between *Drosophila* and *Tribolium* (Fig. 6I) (Bogaert et al., 1987; Wehrli et al., 1993). In *Tribolium*, but not *Drosophila*, however, the genes encoding the basement-membrane component Laminin B1 and Dystroglycan (another ECM receptor) are upregulated in the presumptive mesoderm (Fig. 6N and Fig. 7K; Table S8, data not shown) (Dekkers et al., 2004; Montell and Goodman, 1989; Schneider and Baumgartner, 2008; Urbano et al., 2009). The interaction of laminin with surface receptors like integrins and dystroglycan plays an important role in gastrulation in many organisms, in particular in vertebrates (Ettensohn and Winkelbauer, 2004). Thus, the early expression of these components in *Tribolium* might indicate an ancestral feature of ventral furrow formation which has been partially lost in *Drosophila*. Although the *Tc-LanB1* knockdown does not abolish ventral furrow formation, it might influence its kinetics. The earliest phenotypes we observed are morphological defects in the posterior germ band. In late embryos, the body wall muscles are highly disorganized (Fig. S5). Thus, in *Tribolium*, *LanB1* is required earlier than in *Drosophila* for correct morphogenesis and the late embryonic knockdown phenotypes appear to be much stronger than the *LanB1* mutant phenotypes of *Drosophila*, which show rather mild muscle defects (Urbano et al., 2009).

One of the most interesting genes we have found is *Tc-zfh1*. This gene had also been identified through differential transcriptome analysis in *Drosophila* (Casal and Leptin, 1996). It was first described because it codes for an unusual transcription factor combining zinc fingers and a homeodomain (Casal and Leptin, 1996; Fortini et al., 1991; Lai et al., 1991). The *Drosophila zfh1* mutants show weak somatic muscle phenotypes (Lai et al., 1993), lack the CVM and have defects in the gonadal mesoderm (Broihier et al., 1998; Kusch and Reuter, 1999). *Tc-zfh1* knockdown leads to multiple morphogenetic defects during germ band formation. Most importantly, however, *Tc-zfh1* is required for maintaining *Tc-twi* expression and thus is an essential component for mesoderm development in *Tribolium*.

In conclusion, by studying subsets of genes differentially expressed after manipulating DV patterning in *Tribolium* we have succeeded in identifying components of the *Tribolium* DV-GRN in an unbiased way. The dataset presented here will be screened for further candidates and will serve as a strong foundation for more detailed studies on a wide range of questions surrounding insect embryo axis patterning, cell fate specification and morphogenesis.

MATERIALS AND METHODS

Strains

The San Bernadino wild-type strain was used for RNAi injections and as wild-type control, if not specified otherwise. For selected experiments, we used pBA19 (Lorenzen et al., 2003), G04609 (Koelzer et al., 2014) and an nGFP strain (Sarrazin et al., 2012).

In situ hybridization

ISH was essentially performed as described previously (van der Zee et al., 2005) and the complete protocol can be found in supplementary Materials and Methods.

RNAi

dsRNA was produced with the MEGAscript T7 Kit (Ambion) according to the manufacturer's protocol. The synthesized dsRNA was purified by phenol chloroform extraction. For all knockdown experiments, with the exception of the *Tc-dpp* knockdown, female pupae were injected with 1 µg/µl dsRNA. For the *Tc-dpp* knockdown adult females were injected. For *TC011114*, phenotypes were too strong after injection of 1 µg/µl and we injected 0.5 µg/µl and 0.1 µg/µl instead. For off-target analysis of primers and RNA fragments used to produce dsRNA, see Table S10.

RNA sequencing and analysis for differential expression

Total RNA was isolated using TRIzol reagent (Invitrogen) from a batch of embryos staged to 7.5 h to 11.5 h after egg lay at 30°C. See supplementary Materials and Methods for a step-by-step protocol of RNA isolation. The knockdown efficiency was evaluated by qRT-PCR for each individual RNA sample (e.g. see Fig. S1). Five biological replicates for each *Tc-Toll* knockdown, *Tc-twist* knockdown and wild-type embryos and three biological replicates for each *Tc-sog*, *Tc-dpp* and *dsRed* knockdown embryos were sequenced in 100 bp mode on a HiSeq 2000 (Illumina) by the Cologne Center for Genomics (CCG, paired-end mode) or by GATC Biotech (Konstanz, single-end mode). Biases introduced by sequencing different samples in different sequencing facilities were detected by a principle component analysis (data not shown) and considered in all downstream analyses. Quality of the FASTQ formatted sequences was verified using FastQC (v.3.5.12; www.bioinformatics.babraham.ac.uk/projects/fastqc/). Bowtie2 (v.2.0.2; bowtie-bio.sourceforge.net/bowtie2) with 'very sensitive' settings used in Tophat (ccb.jhu.edu/software/tophat/) to map the sequences to the Tcas3.0 gene set. The data have been submitted to NCBI under accession number PRJNA315762. Count tables that summarize reads per gene were compiled in R (v.3.0.2 2013-09-25, accessed with RStudio v.0.97.551) using either the 'countOverlaps' function from the IRanges (v. ≥1.18.2; bioconductor.org/packages/release/bioc/html/IRanges.html) package (for subsequent processing with edgeR) or the 'summarizedOverlaps' function in mode 'union' from GenomicRanges (v.1.12.4; bioconductor.org/packages/release/bioc/html/GenomicRanges.html) (for subsequent processing with DESeq2). The data were then tested for differentially expressed genes with edgeR (v.3.2.4; bioconductor.org/packages/release/bioc/html/edgeR.html) and DESeq2 (v.1.0.18; bioconductor.org/packages/release/bioc/html/DESeq2.html) (Anders and Huber, 2010; Robinson et al., 2010). The edgeR analysis was essentially performed as described in section 4.5 of the edgeR Users Guide (31 March 2013). The DESeq analysis was performed as described in the Analyzing RNA-Seq data with the DESeq2 package manual (15 July 2013), with the exception that the function 'nbinomWaldTest' was used without using a cut-off for Cook's distance. Only genes that were detected to be differentially expressed by both algorithms at a 5% FDR were considered to be differentially expressed.

qRT-PCR

The efficiency of RNAi treatment was evaluated with qRT-PCR prior to transcriptome sequencing. A part of each staged RNA batch isolated from knockdown and wild-type embryos was transcribed into cDNA using SuperScriptVILO cDNA Synthesis Kit (Life Technologies). Quantities of the knocked down genes or their target genes were compared between offspring from dsRNA-injected mothers and wild-type embryos using SYBR Green (Applied Biosystems) and a 7500 Fast Real-time PCR system (Applied Biosystems). The reaction volume was 25 µl (12.5 µl SYBR Green PCR master mix, 2 µl cDNA, 1 µl forward primer, 1 µl reverse primer, 8.5 µl H_2O) and the cycling profile was: 94°C 5 min, 35 cycles of 94°C 30 s, 55°C 30 s, 72°C 1 min and extension at 72°C for 5 min. The amplification efficiency for each primer pair was empirically determined in each qRT-PCR run and for calculation of the RNA ratios from knockdown embryos and wild-type embryos the ΔCt method was used. See primer list for primer sequences.

Development (2016) 143, 2443-2454 doi:10.1242/dev.130641

Live imaging

Live imaging was performed with dechorionated embryos mounted on slides and immersed in Halocarbon oil 700 (Sigma) on an Applied Precision DeltaVision RT wide-field microscope at 30°C. Movies were generated using an ImageJ macro created by Thorsten Horn (Institute of Developmental Biology, University of Cologne).

Histochemistry

DAPI and Phalloidin staining were carried out using standard methods as detailed in supplementary Materials and Methods. Antibody staining for phosphotyrosine was performed using 1:500 monoclonal anti-phosphotyrosine (Sigma, P3300) and 1:400 goat anti-mouse secondary antibody, Alexa Fluor 555 conjugate (Thermo Fisher Scientific, A-21422).

Primers

Full list of primers used is shown in Table S9.

Acknowledgements

We are especially grateful to Rodrigo Nunes da Fonseca and Jeremy A. Lynch for advice and discussions. We thank Thorsten Horn for his help with live imaging, and Matt Benton, Matthias Pechmann and Waldemar Wojciech for valuable comments on the manuscript and for corrections.

Competing interests

The authors declare no competing or financial interests.

Author contributions

D.S., N.F. and S.R. designed research; N.F. and D.S. performed RNA-seq experiments; D.S. analysed data bioinformatically; N.F. and D.S. performed downstream analysis; C.v.L. initially described the *Tc-twist* phenotype; D.S., N.F. and S.R. wrote the manuscript. All authors approved the final version of the manuscript.

Funding

We thank the Deutsche Forschungsgemeinschaft (DFG) for funding this project as part of the Collaborative Research Grant SFB 680, 'Molecular Basis of Evolutionary Innovations' and Boehringer Ingelheim Fonds for supporting D.S. with a BIF PhD Fellowship. We further thank the International Graduate School for Genetics and Functional Genomics (Cologne) for supporting C.v.L. and the International Graduate School in Development Health and Disease (Cologne) for supporting N.F., D.S. and this work.

Data availability

RNA-seq data have been submitted to NCBI under accession number PRJNA315762 and can be accessed at: http://www.ncbi.nlm.nih.gov/bioproject/?term=PRJNA315762.

Supplementary information

Supplementary information available online at http://dev.biologists.org/lookup/doi/10.1242/dev.130641.supplemental

References

Anders, S. and Huber, W. (2010). Differential expression analysis for sequence count data. *Genome Biol.* **11**, R106.

Aranda, M., Marques-Souza, H., Bayer, T. and Tautz, D. (2008). The role of the segmentation gene hairy in Tribolium. *Dev. Genes Evol.* **218**, 465-477.

Bardin, A. J. and Schweisguth, F. (2006). Bearded family members inhibit Neuralized-mediated endocytosis and signaling activity of Delta in Drosophila. *Dev. Cell* **10**, 245-255.

Beermann, A. and Schröder, R. (2008). Sites of Fgf signalling and perception during embryogenesis of the beetle Tribolium castaneum. *Dev. Genes Evol.* **218**, 153-167.

Beiman, M., Shilo, B. Z. and Volk, T. (1996). Heartless, a Drosophila FGF receptor homolog, is essential for cell migration and establishment of several mesodermal lineages. *Genes Dev.* **10**, 2993-3002.

Benton, M. A., Akam, M. and Pavlopoulos, A. (2013). Cell and tissue dynamics during Tribolium embryogenesis revealed by versatile fluorescence labeling approaches. *Development* **140**, 3210-3220.

Berghammer, A., Bucher, G., Maderspacher, F. and Klingler, M. (1999). A system to efficiently maintain embryonic lethal mutations in the flour beetle *Tribolium castaneum*. *Dev. Genes Evol.* **209**, 382-389.

Berghammer, A. J., Weber, M., Trauner, J. and Klingler, M. (2009). Red flour beetle (Tribolium) germline transformation and insertional mutagenesis. *Cold Spring Harb. Protoc.* **2009**, pdb.prot5259.

Biffar, L. and Stollewerk, A. (2014). Conservation and evolutionary modifications of neuroblast expression patterns in insects. *Dev. Biol.* **388**, 103-116.

Bogaert, T., Brown, N. and Wilcox, M. (1987). The Drosophila PS2 antigen is an invertebrate integrin that, like the fibronectin receptor, becomes localized to muscle attachments. *Cell* **51**, 929-940.

Broihier, H. T., Moore, L. A., Van Doren, M., Newman, S. and Lehmann, R. (1998). zfh-1 is required for germ cell migration and gonadal mesoderm development in Drosophila. *Development* **125**, 655-666.

Brown, S. J., Patel, N. H. and Denell, R. E. (1994). Embryonic expression of the single Tribolium engrailed homolog. *Dev. Genet.* **15**, 7-18.

Casal, J. and Leptin, M. (1996). Identification of novel genes in Drosophila reveals the complex regulation of early gene activity in the mesoderm. *Proc. Natl. Acad. Sci. USA* **93**, 10327-10332.

Chang, Z., Price, B. D., Bockheim, S., Boedigheimer, M. J., Smith, R. and Laughon, A. (1993). Molecular and genetic characterization of the Drosophila tartan gene. *Dev. Biol.* **160**, 315-332.

Chen, G., Handel, K. and Roth, S. (2000). The maternal NF-kappaB/dorsal gradient of *Tribolium castaneum*: dynamics of early dorsoventral patterning in a short-germ beetle. *Development* **127**, 5145-5156.

Choe, C. P. and Brown, S. J. (2007). Evolutionary flexibility of pair-rule patterning revealed by functional analysis of secondary pair-rule genes, paired and sloppy-paired in the short-germ insect, *Tribolium castaneum*. *Dev. Biol.* **302**, 281-294.

Davis, G. K., Jaramillo, C. A. and Patel, N. H. (2001). Pax group III genes and the evolution of insect pair-rule patterning. *Development* **128**, 3445-3458.

De Renzis, S., Yu, J., Zinzen, R. and Wieschaus, E. (2006). Dorsal-ventral pattern of Delta trafficking is established by a Snail-Tom-Neuralized pathway. *Dev. Cell* **10**, 257-264.

Dekkers, L. C., van der Plas, M. C., van Loenen, P. B., den Dunnen, J. T., van Ommen, G.-J. B., Fradkin, L. G. and Noordermeer, J. N. (2004). Embryonic expression patterns of the Drosophila dystrophin-associated glycoprotein complex orthologs. *Gene Expr. Patterns* **4**, 153-159.

Donitz, J., Schmitt-Engel, C., Grossmann, D., Gerischer, L., Tech, M., Schoppmeier, M., Klingler, M. and Bucher, G. (2015). iBeetle-Base: a database for RNAi phenotypes in the red flour beetle *Tribolium castaneum*. *Nucleic Acids Res.* **43**, D720-D725.

Ettensohn, C. A. and Winkelbauer, R. (2004). Cell-substrate interactions during deuterostome gastrulation. In *Gastrulation* (ed. C.D. Stern), pp. 317-328. Cold Spring Harbor, New York: Cold Spring Harbor Laboratory Press.

Farzana, L. and Brown, S. J. (2008). Hedgehog signaling pathway function conserved in Tribolium segmentation. *Dev. Genes Evol.* **218**, 181-192.

Fonseca, R. N., Lynch, J. A. and Roth, S. (2009). Evolution of axis formation: mRNA localization, regulatory circuits and posterior specification in non-model arthropods. *Curr. Opin. Genet Dev.* **19**, 404-411.

Fortini, M. E., Lai, Z. C. and Rubin, G. M. (1991). The Drosophila zfh-1 and zfh-2 genes encode novel proteins containing both zinc-finger and homeodomain motifs. *Mech. Dev.* **34**, 113-122.

Francois, V., Solloway, M., O'Neill, J. W., Emery, J. and Bier, E. (1994). Dorsal-ventral patterning of the Drosophila embryo depends on a putative negative growth factor encoded by the short gastrulation gene. *Genes Dev.* **8**, 2602-2616.

Gisselbrecht, S., Skeath, J. B., Doe, C. Q. and Michelson, A. M. (1996). Heartless encodes a fibroblast growth factor receptor (DFR1/DFGF-R2) involved in the directional migration of early mesodermal cells in the Drosophila embryo. *Genes Dev.* **10**, 3003-3017.

Handel, K., Basal, A., Fan, X. and Roth, S. (2005). *Tribolium castaneum* twist: gastrulation and mesoderm formation in a short-germ beetle. *Dev. Genes Evol.* **215**, 13-31.

Hong, J.-W., Hendrix, D. A., Papatsenko, D. and Levine, M. S. (2008). How the Dorsal gradient works: insights from postgenome technologies. *Proc. Natl. Acad. Sci. USA* **105**, 20072-20076.

Imam, F., Sutherland, D., Huang, W. and Krasnow, M. A. (1999). Stumps, a Drosophila gene required for fibroblast growth factor (FGF)-directed migrations of tracheal and mesodermal cells. *Genetics* **152**, 307-318.

Jazwinska, A., Rushlow, C. and Roth, S. (1999). The role of brinker in mediating the graded response to Dpp in early Drosophila embryos. *Development* **126**, 3323-3334.

King, B. and Denholm, B. (2014). Malpighian tubule development in the red flour beetle (*Tribolium castaneum*). *Arthropod. Struct. Dev.* **43**, 605-613.

Knust, E., Schrons, H., Grawe, F. and Campos-Ortega, J. A. (1992). Seven genes of the Enhancer of split complex of Drosophila melanogaster encode helix-loop-helix proteins. *Genetics* **132**, 505-518.

Koelzer, S., Kölsch, Y. and Panfilio, K. A. (2014). Visualizing late insect embryogenesis: extraembryonic and mesodermal enhancer trap expression in the beetle *Tribolium castaneum*. *PLoS ONE* **9**, e103967.

Kusch, T. and Reuter, R. (1999). Functions for Drosophila brachyenteron and forkhead in mesoderm specification and cell signalling. *Development* **126**, 3991-4003.

Kux, K., Kiparaki, M. and Delidakis, C. (2013). The two Tribolium E(spl) genes show evolutionarily conserved expression and function during embryonic neurogenesis. *Mech. Dev.* **130**, 207-225.

Lai, Z. C., Fortini, M. E. and Rubin, G. M. (1991). The embryonic expression patterns of zfh-1 and zfh-2, two Drosophila genes encoding novel zinc-finger homeodomain proteins. *Mech. Dev.* **34**, 123-134.
Lai, Z. C., Rushton, E., Bate, M. and Rubin, G. M. (1993). Loss of function of the Drosophila zfh-1 gene results in abnormal development of mesodermally derived tissues. *Proc. Natl. Acad. Sci. USA* **90**, 4122-4126.
Leulier, F. and Lemaitre, B. (2008). Toll-like receptors — taking an evolutionary approach. *Nat. Rev. Genet.* **9**, 165-178.
Lorenzen, M. D., Berghammer, A. J., Brown, S. J., Denell, R. E., Klingler, M. and Beeman, R. W. (2003). piggyBac-mediated germline transformation in the beetle *Tribolium castaneum*. *Insect Mol. Biol.* **12**, 433-440.
Loubéry, S., Seum, C., Moraleda, A., Daeden, A., Fürthauer, M. and Gonzalez-Gaitan, M. (2014). Uninflatable and Notch control the targeting of Sara endosomes during asymmetric division. *Curr. Biol.* **24**, 2142-2148.
Lynch, J. A. and Roth, S. (2011). The evolution of dorsal-ventral patterning mechanisms in insects. *Genes Dev.* **25**, 107-118.
Milán, M., Weihe, U., Pérez, L. and Cohen, S. M. (2001). The LRR proteins capricious and Tartan mediate cell interactions during DV boundary formation in the Drosophila wing. *Cell* **106**, 785-794.
Milán, M., Pérez, L. and Cohen, S. M. (2005). Boundary formation in the Drosophila wing: functional dissection of Capricious and Tartan. *Dev. Dyn.* **233**, 804-810.
Montell, D. J. and Goodman, C. S. (1989). Drosophila laminin: sequence of B2 subunit and expression of all three subunits during embryogenesis. *J. Cell Biol.* **109**, 2441-2453.
Nunes da Fonseca, R., von Levetzow, C., Kalscheuer, P., Basal, A., van der Zee, M. and Roth, S. (2008). Self-regulatory circuits in dorsoventral axis formation of the short-germ beetle *Tribolium castaneum*. *Dev. Cell* **14**, 605-615.
Nunes da Fonseca, R., van der Zee, M. and Roth, S. (2010). Evolution of extracellular Dpp modulators in insects: the roles of tolloid and twisted-gastrulation in dorsoventral patterning of the Tribolium embryo. *Dev. Biol.* **345**, 80-93.
O'Connor, M. B., Umulis, D., Othmer, H. G. and Blair, S. S. (2006). Shaping BMP morphogen gradients in the Drosophila embryo and pupal wing. *Development* **133**, 183-193.
Ozdemir, A., Ma, L., White, K. P. and Stathopoulos, A. (2014). Su(H)-mediated repression positions gene boundaries along the dorsal-ventral axis of Drosophila embryos. *Dev. Cell* **31**, 100-113.
Özüak, O., Buchta, T., Roth, S. and Lynch, J. A. (2014). Dorsoventral polarity of the Nasonia embryo primarily relies on a BMP gradient formed without input from Toll. *Curr. Biol.* **24**, 2393-2398.
Reeves, G. T. and Stathopoulos, A. (2009). Graded dorsal and differential gene regulation in the Drosophila embryo. *Cold Spring Harb. Perspect. Biol.* **1**, a000836.
Reeves, G. T., Trisnadi, N., Truong, T. V., Nahmad, M., Katz, S. and Stathopoulos, A. (2012). Dorsal-ventral gene expression in the Drosophila embryo reflects the dynamics and precision of the dorsal nuclear gradient. *Dev. Cell* **22**, 544-557.
Robinson, M. D., McCarthy, D. J. and Smyth, G. K. (2010). edgeR: a Bioconductor package for differential expression analysis of digital gene expression data. *Bioinformatics* **26**, 139-140.
Roth, S., Stein, D. and Nüsslein-Volhard, C. (1989). A gradient of nuclear localization of the dorsal protein determines dorsoventral pattern in the Drosophila embryo. *Cell* **59**, 1189-1202.
Rushlow, C. A., Han, K., Manley, J. L. and Levine, M. (1989). The graded distribution of the dorsal morphogen is initiated by selective nuclear transport in Drosophila. *Cell* **59**, 1165-1177.
Sachs, L., Chen, Y.-T., Drechsler, A., Lynch, J. A., Panfilio, K. A., Lässig, M., Berg, J. and Roth, S. (2015). Dynamic BMP signaling polarized by Toll patterns the dorsoventral axis in a hemimetabolous insect. *eLife* **4**, e05502.
Sarrazin, A. F., Peel, A. D. and Averof, M. (2012). A segmentation clock with two-segment periodicity in insects. *Science* **336**, 338-341.
Schmitt-Engel, C., Schultheis, D., Schwirz, J., Ströhlein, N., Troelenberg, N., Majumdar, U., Dao, V. A., Grossmann, D., Richter, T., Tech, M. et al. (2015). The iBeetle large-scale RNAi screen reveals gene functions for insect development and physiology. *Nat. Commun.* **6**, 7822.
Schneider, M. and Baumgartner, S. (2008). Differential expression of Dystroglycan-spliceforms with and without the mucin-like domain during Drosophila embryogenesis. *Fly* **2**, 29-35.
Sharma, R., Beer, K., Iwanov, K., Schmöhl, F., Beckmann, P. I. and Schröder, R. (2015). The single fgf receptor gene in the beetle *Tribolium castaneum* codes for two isoforms that integrate FGF8- and Branchless-dependent signals. *Dev. Biol.* **402**, 264-275.
Simpson, P. (1983). Maternal-zygotic gene interactions during formation of the dorsoventral pattern in Drosophila embryos. *Genetics* **105**, 615-632.
Stein, D. S. and Stevens, L. M. (2014). Maternal control of the Drosophila dorsal-ventral body axis. *Wiley Interdiscip. Rev. Dev. Biol.* **3**, 301-330.
Steward, R. (1989). Relocalization of the dorsal protein from the cytoplasm to the nucleus correlates with its function. *Cell* **59**, 1179-1188.
Ungerer, P., Eriksson, B. J. and Stollewerk, A. (2011). Neurogenesis in the water flea *Daphnia magna* (Crustacea, Branchiopoda) suggests different mechanisms of neuroblast formation in insects and crustaceans. *Dev. Biol.* **357**, 42-52.
Urbano, J. M., Torgler, C. N., Molnar, C., Tepass, U., Lopez-Varea, A., Brown, N. H., de Celis, J. F. and Martin-Bermudo, M. D. (2009). Drosophila laminins act as key regulators of basement membrane assembly and morphogenesis. *Development* **136**, 4165-4176.
van der Zee, M., Berns, N. and Roth, S. (2005). Distinct functions of the *Tribolium zerknullt* genes in serosa specification and dorsal closure. *Curr. Biol.* **15**, 624-636.
van der Zee, M., Stockhammer, O., von Levetzow, C., Nunes da Fonseca, R. and Roth, S. (2006). Sog/Chordin is required for ventral-to-dorsal Dpp/BMP transport and head formation in a short germ insect. *Proc. Natl. Acad. Sci. USA* **103**, 16307-16312.
Vassin, H., Bremer, K. A., Knust, E. and Campos-Ortega, J. A. (1987). The neurogenic gene Delta of *Drosophila melanogaster* is expressed in neurogenic territories and encodes a putative transmembrane protein with EGF-like repeats. *EMBO J.* **6**, 3431-3440.
Vincent, S., Wilson, R., Coelho, C., Affolter, M. and Leptin, M. (1998). The Drosophila protein Dof is specifically required for FGF signaling. *Mol. Cell* **2**, 515-525.
Wang, Y.-C. and Ferguson, E. L. (2005). Spatial bistability of Dpp–receptor interactions during Drosophila dorsal–ventral patterning. *Nature* **434**, 229-234.
Wech, I., Bray, S., Delidakis, C. and Preiss, A. (1999). Distinct expression patterns of different enhancer of split bHLH genes during embryogenesis of *Drosophila melanogaster*. *Dev. Genes Evol.* **209**, 370-375.
Wehrli, M., DiAntonio, A., Fearnley, I. M., Smith, R. J. and Wilcox, M. (1993). Cloning and characterization of alpha PS1, a novel *Drosophila melanogaster* integrin. *Mech. Dev.* **43**, 21-36.
Wheeler, S. R., Carrico, M. L., Wilson, B. A., Brown, S. J. and Skeath, J. B. (2003). The expression and function of the achaete-scute genes in *Tribolium castaneum* reveals conservation and variation in neural pattern formation and cell fate specification. *Development* **130**, 4373-4381.
Xie, G., Zhang, H., Du, G., Huang, Q., Liang, X., Ma, J. and Jiao, R. (2012). Uif, a large transmembrane protein with EGF-like repeats, can antagonize Notch signaling in Drosophila. *PLoS ONE* **7**, e36362.
Yang, X., ZarinKamar, N., Bao, R. and Friedrich, M. (2009). Probing the Drosophila retinal determination gene network in Tribolium (I): The early retinal genes dachshund, eyes absent and sine oculis. *Dev. Biol.* **333**, 202-214.
Zhang, L. and Ward, R. E. (2009). Uninflatable encodes a novel ectodermal apical surface protein required for tracheal inflation in Drosophila. *Dev. Biol.* **336**, 201-212.